J|A|C|S
ARTICLES
Published on Web 11/18/2006

Binding of Muscimol-Conjugated Quantum Dots to $GABA_C$ Receptors

Hélène A. Gussin,[†] Ian D. Tomlinson,[§] Deborah M. Little,[‡] Michael R. Warnement,[§] Haohua Qian,[†] Sandra J. Rosenthal,[§] and David R. Pepperberg*,[†]

Contribution from the Lions of Illinois Eye Research Institute, Department of Ophthalmology and Visual Sciences, Department of Neurology and Rehabilitation, and Center for Cognitive Medicine, University of Illinois at Chicago, Chicago, Illinois 60612, and Department of Chemistry, Vanderbilt University, Nashville, Tennessee 37232

Received June 19, 2006; E-mail: davipepp@uic.edu

Abstract: Functionalization of highly fluorescent CdSe/ZnS core−shell nanocrystals (quantum dots, qdots) is an emerging technology for labeling cell surface proteins. We have synthesized a conjugate consisting of ∼150−200 muscimols (a GABA receptor agonist) covalently joined to the qdot via a poly(ethylene glycol) (PEG) linker (∼78 ethylene glycol units) and investigated the binding of this muscimol−PEG−qdot conjugate to homomeric ρ1 $GABA_C$ receptors expressed in *Xenopus* oocytes. $GABA_C$ receptors mediate inhibitory synaptic signaling at multiple locations in the central nervous system (CNS). Binding of the conjugate was analyzed quantitatively by determining the fluorescence intensity of the oocyte surface membrane in relation to that of the surrounding incubation medium. Upon 5- to 10-min incubation with muscimol−PEG−qdots (34 nM in qdot concentration), $GABA_C$-expressing oocytes exhibited a fluorescent halo at the surface membrane that significantly exceeded the fluorescence of the incubation medium. This halo was absent following muscimol−PEG−qdot treatment of oocytes lacking $GABA_C$ receptors. Incubation of the oocyte with free muscimol (100 μM−5 mM), PEG−muscimol (500 μM), or GABA (100 μM − 5 mM) substantially reduced or eliminated the fluorescence halo produced by muscimol−PEG−qdots, and the removal of GABA or free muscimol led to a recovery of muscimol−PEG−qdot binding. Unconjugated qdots and PEG−qdots that lacked conjugated muscimol neither exhibited significant binding activity nor diminished the subsequent binding of muscimol−PEG−qdots. The results indicate that muscimol joined to qdots via a long-chain PEG linker exhibits specific binding activity at the ligand-binding pocket of expressed $GABA_C$ receptors, despite the presence of both the long PEG linker and the sterically bulky qdot.

Introduction

Fluorescent nanocrystals, or quantum dots (qdots), have shown great promise as biological imaging agents since their introduction in 1998.[1,2] They have many inherent advantages over conventional fluorophores.[2−5] Specifically, their higher quantum yields, photostability, size-tunable, narrow emission spectra, and continuous absorption spectrum make them ideally suited for highly sensitive, multiplexed, dynamic imaging. Various examples of biological imaging with qdots have been reported,[6] including whole cell assays[2] and imaging applications in vivo.[7]

For efficient biolabeling by a qdot-containing preparation, the qdots must maintain three properties under aqueous conditions: efficient fluorescence, colloidal stability, and low nonspecific adsorption. A variety of techniques have been used to achieve these goals, including encapsulation in micelles,[8] silanization,[9] encapsulation in amphiphilic polymers,[10,11] and encapsulation in proteins such as avidin and streptavidin.[12] Biological activity is introduced by conjugating ligands that have the desired biological effect. A variety of biologically active ligands have been linked to qdots, such as proteins,[13−18]

[†] Lions of Illinois Eye Research Institute, University of Illinois at Chicago.
[‡] Department of Neurology and Rehabilitation, University of Illinois at Chicago.
[§] Vanderbilt University.

(1) Bruchez, M., Jr.; Moronne, M.; Gin, P.; Weiss, S.; Alivisatos, A. P. *Science* **1998**, *281*, 2013−2016.
(2) Chan, W. C. W.; Nie, S. *Science* **1998**, *281*, 2016−2018.
(3) Alivisatos, A. P. *J. Phys. Chem.* **1996**, *100*, 13226−13239.
(4) Murray, C. B.; Norris, D. J.; Bawendi, M. G. *J. Am. Chem. Soc.* **1993**, *115*, 8706−8715.
(5) Hines, M. A.; Guyot-Sionnest, P. *J. Phys. Chem.* **1996**, *100*, 468−471.
(6) Alivisatos, P. *Nat. Biotechnol.* **2004**, *22*, 47−52.
(7) Kim, S.; Lim, Y. T.; Soltesz, E. G.; De Grand, A. M.; Lee, J.; Nakayama, A.; Parker, J. A.; Mihaljevic, T.; Laurence, R. G.; Dor, D. M.; Cohn, L. H.; Bawendi, M. G.; Frangioni, J. V. *Nat. Biotechnol.* **2004**, *22*, 93−97.
(8) Dubertret, B.; Skourides, P.; Norris, D. J.; Noireaux, V.; Brivanlou, A. H.; Libchaber, A. *Science* **2002**, *298*, 1759−1762.
(9) Gerion, D.; Pinaud, F.; Williams, S. C.; Parak, W. J.; Zanchet, D.; Weiss, S.; Alivisatos, A. P. *J. Phys. Chem.* **2001**, *105*, 8861−8871.
(10) Jovin, T. M. *Nat. Biotechnol.* **2003**, *21*, 32−33.
(11) Gao, X.; Cui, Y.; Levenson, R. M.; Chung, L. W. K.; Nie, S. *Nat. Biotechnol.* **2004**, *22*, 969−976.
(12) Wu, X.; Liu, H.; Liu, J.; Haley, K. N.; Treadway, J. A.; Larson, J. P.; Ge, N.; Peale, F.; Bruchez, M. P. *Nat. Biotechnol.* **2003**, *21*, 41−46.
(13) Chunyang, Z.; Hui, M.; Yao, D.; Lei, J.; Dieyan, C.; Shuming, N. *Analyst* **2000**, *125*, 1029−1031.
(14) Hoshino, A.; Hanaki, K.; Suzuki, K.; Yamamoto, K. *Biochem. Biophys. Res. Commun.* **2004**, *314*, 46−53.
(15) Bäumle, M.; Stamou, D.; Segura, J.; Hovius, J.; Vogel, H. *Langmuir* **2004**, *20*, 3828−3831.
(16) Michalet, X.; Pinaud, F.; Lacoste, T. D.; Dahan, M.; Bruchez, M. P.; Alivisatos, A. P.; Weiss, S. *Single Mol.* **2001**, *2*, 261−276.

peptides,[19,20] and antibodies.[11,12,21−23] The most common method used for this conjugation is the attachment of biotin to the biologically active molecule, followed by attachment of the biotinylated ligand to streptavidin-coated qdots. For example, Dahan et al.[23] have reported the use of biotinylated antibodies and streptavidin−qdots, to target glycine receptors and achieve dynamic imaging of live cells.

A distinct approach to achieving bioactivity of a qdot-containing structure is to synthesize derivatives of biologically active small molecules[24−27] and attach them to the qdot. Neurotransmitters and other small molecules that interact with cells of the central nervous system (CNS) are of particular interest in this regard. In an earlier study, specific labeling of the serotonin transporter protein using serotonin-conjugated qdots was demonstrated.[28] The present study further develops the use of small molecule-conjugated qdots as probes for postsynaptic membrane receptors. Specifically, we have employed quantitative fluorescence imaging to examine the binding, to neurotransmitter receptors expressed in a model cell system, of a novel qdot conjugate containing an agonist for the receptor. In the investigated qdot conjugate, the receptor agonist is joined, via a poly(ethylene glycol) (PEG) chain and an amide linkage, to CdSe/ZnS core−shell qdots coated with a modified polyacrylamide (AMP) polymer. Use of the PEG linker was motivated by earlier findings[29] indicating that PEGylation of the qdot reduces nonspecific binding of the resulting conjugate to cell surfaces.

The neurotransmitter receptor selected for the present investigation is the $GABA_C$ receptor, a ligand-gated ion channel that in vivo is activated by the neurotransmitter γ-aminobutyric acid (GABA). $GABA_C$ receptors are expressed in the retina and in many other regions of the CNS.[30−36] Native $GABA_C$ receptors are pentameric and consist of a heteromeric combination of GABA ρ subunits.[37−39] However, $GABA_C$ subunits are capable of forming fully functional homopentamers when expressed in model cell systems such as *Xenopus* oocytes;[40−42] the homopentamer structure is of advantage in that it simplifies both receptor expression and the analysis of binding. Muscimol (5-aminomethyl-3-hydroxyisoxazole) is a well-known agonist of $GABA_C$ receptors (as well as of $GABA_A$ receptors, another GABA-responsive postsynaptic receptor widely distributed in the CNS). The present experiments show that a conjugate consisting of muscimol joined to AMP qdots through an aminohexanoyl linker and PEG 3400 chain exhibits robust and specific binding to $GABA_C$ receptors expressed in *Xenopus* oocytes.

Experimental Section

Chemical Synthesis and Characterization. A. Materials. AMP-coated CdSe/ZnS core−shell qdots with maximum fluorescence emission at 605 nm were a gift from Quantum Dot Corporation (Haywood, CA) and were supplied as an 8.4 μM solution in borate buffer (pH 8.5). The same AMP-coated qdots are now available from Invitrogen (Invitrogen Corporation, Carlsbad, CA) and referred to as the Qdot Innovator's Tool Kit ITK nanocrystals. *tert*-Butyloxycarbonyl (BOC) amine-poly(ethylene glycol)-*N*-hydroxysuccinimide ester (BOC-NH-PEG-NHS; purity >85%) was obtained from Nektar Therapeutics (Huntsville, AL). The poly(ethylene glycol) (PEG) chains of this product had a molecular weight (determined by MALDI) of 3446 Da (approximately 78 ethylene glycol units) and a polydispersity of 1.00. Unless otherwise indicated, the term "PEG" used throughout the present text denotes a PEG chain consisting of about 78 ethylene glycol units. Trifluoroacetic acid (TFA), *N*-hydroxy succinimide (NHS), 1-[3-(dimethylamino)propyl]-3-ethylcarbodiimide hydrochloride (EDC), *p*-toluenesulfonyl chloride, hydrazine hydrate, and pyridine were obtained from Aldrich Chemical Corporation (Milwaukee, WI). Methylene chloride, acetonitrile, ethanol, and methanol were obtained from Fischer Scientific (Fair Lawn, NJ) and used without purification. Potassium phthalimide was obtained from Lancaster Synthesis (Windham, NH). Sodium hydroxide and magnesium sulfate were obtained from VWR International (West Chester, PA). PEG 2000 monomethyl ether [poly(ethylene glycol) chains of molecular weight ~2000 Da on average (polydispersity of 1.07; molecular weight range of 1895−2167 Da)] was obtained from Fluka/Sigma-Aldrich, St. Louis, MO. Borate buffer was obtained from Poly Sciences Inc. (Warrington, PA) as a 5X concentrate and diluted to 1X before use. Sephadex G-50 was obtained from Amersham Biosciences (Uppsala, Sweden). All other reagents were used as supplied unless otherwise stated.

B. Overview of Preparation of qdot Conjugates. The primary structure synthesized for investigation was a CdSe/ZnS qdot preparation functionalized to contain multiple copies of the $GABA_C$ agonist muscimol. Each muscimol group was joined to the qdot through a short (6-aminohexanoyl; AH) spacer and a PEG 3400 linker (Figure 1). Muscimol, synthesized as described by Frey and Jäger,[43] was attached to the AH spacer by reaction with 6-*tert*-butoxycarboxamido-hexanoic acid *N*-hydroxysuccinimide ester (BOC-AH-NHS, synthesized as described by Doughty et al.[44]), yielding compound **1** in Figure 2. After removal of the BOC protecting group with TFA, the resulting AH-muscimol (**2**) was coupled to BOC-NH-PEG-CONHS. Removal of the BOC group of the product (**3**) with TFA provided NH_2−PEG−AH-muscimol (**4**), henceforth termed "PEG−muscimol". The PEG−muscimol was conjugated to terminating carboxyl groups on the AMP-coated qdots using 1-[3-(dimethylamino)propyl]-3-ethylcarbodiimide

(17) Goldman, E. R.; Balighian, E. D.; Mattoussi, H.; Kuno, K. M.; Mauro, J. M.; Tran, P. T.; Anderson, G. P. *J. Am. Chem. Soc.* **2002**, *124*, 6378−6382.
(18) Minet, O.; Dressler, C.; Beuthan, J. *J. Fluoresc.* **2004**, *14*, 241−247.
(19) Åkerman, M. E.; Chan, W. C. W.; Laakkonen, P.; Bhatia, S. N.; Ruoslahti, E. *Proc. Natl. Acad. Sci. U.S.A.* **2002**, *99*, 12617−12621.
(20) Lidke, D. S.; Nagy, P.; Heintzmann, R.; Arndt-Jovin, D. J.; Post, J. N.; Grecco, H. E.; Jares-Erijman, E. A.; Jovin, T. M. *Nat. Biotechnol.* **2004**, *22*, 198−203.
(21) Watson, A.; Wu, X.; Bruchez, M. *Biotechniques* **2003**, *34*, 296−303.
(22) Goldman, E. R.; Clapp, A. R.; Anderson, G. P.; Uyeda, H. T.; Mauro, J. M.; Medintz, I. L.; Mattoussi, H. *Anal. Chem.* **2004**, *76*, 684−688.
(23) Dahan, M.; Lévi, S.; Luccardini, C.; Rostaing, P.; Riveau, B.; Triller, A. *Science* **2003**, *302*, 442−445.
(24) Tomlinson, I. D.; Mason, J.; Burton, J. N.; Blakely, R.; Rosenthal, S. J. *Tetrahedron* **2003**, *59*, 8035−8047.
(25) Tomlinson, I. D.; Grey, J. L.; Rosenthal, S. J. *Molecules* **2002**, *7*, 777−790.
(26) Tomlinson, I. D.; Mason, J. N.; Blakely, R. D.; Rosenthal, S. J. *Bioorg. Med. Chem. Lett.* **2005**, *15*, 5307−5310.
(27) Tomlinson, I. D.; Kippeny, T.; Swafford, L.; Siddiqui, N.; Rosenthal, S. J. *J. Chem. Res.* **2002**, *5*, 203−204.
(28) Rosenthal, S. J.; Tomlinson, I. D.; Adkins, E. M.; Schroeter, S.; Adams, S.; Swafford, L.; McBride, J.; Wang, Y.; DeFelice, L. J.; Blakely, R. D. *J. Am. Chem. Soc.* **2002**, *124*, 4586−4594.
(29) Bentzen, E. L.; Tomlinson, I. D.; Mason, J.; Gresch, P.; Warnement, M. R.; Wright, D.; Sanders-Busch, E.; Blakely, R.; Rosenthal S. J. *Bioconjugate Chem.* **2005**, *16*, 1488−1494.
(30) Qian, H.; Dowling, J. E. *J. Neurosci.* **1994**, *14*, 4299−4307.
(31) Enz, R.; Brandstätter, J. H.; Wässle, H.; Bormann, J. *J. Neurosci.* **1996**, *16*, 4479−4490.
(32) Euler, T.; Wässle, H. *J. Neurophysiol.* **1998**, *79*, 1384−1395.
(33) Lukasiewicz, P. D.; Shields, C. R. *J. Neurophysiol.* **1998**, *79*, 3157−3167.
(34) Shen, W.; Slaughter, M. M. *J. Physiol.* **2001**, *530*, 55−67.
(35) Gibbs, M. E.; Johnston, G. A. R. *Neuroscience* **2005**, *131*, 567−576.
(36) Lukasiewicz, P. D. *Prog. Brain Res.* **2005**, *147*, 205−218.
(37) Zhang, D.; Pan, Z. H.; Zhang, X.; Brideau, A. D.; Lipton S. A. *Proc. Natl. Acad. Sci. U.S.A.* **1995**, *92*, 11756−11760.
(38) Milligan, C. J.; Buckley, N. J.; Garret, M.; Deuchars, J.; Deuchars, S. A. *J. Neurosci.* **2004**, *24*, 7241−7250.
(39) Pan, Y.; Qian, H. *J. Neurochem.* **2005**, *94*, 482−490.
(40) Qian, H.; Dowling, J. E.; Ripps, H. *J. Neurobiol.* **1998**, *37*, 305−320.
(41) Chebib, M. *Clin. Exp. Pharmacol. Physiol.* **2004**, *31*, 800−804.
(42) Sedelnikova, A.; Smith, C. D.; Zakharkin, S. O.; Davis, D.; Weiss, D. S.; Chang, Y. *J. Biol. Chem.* **2005**, *280*, 1535−1542.
(43) Frey, M.; Jäger, V. *Synthesis* **1985**, 1100−1104.
(44) Doughty, M. B.; Chaurasia, C. S.; Li, K. *J. Med. Chem.* **1993**, *36*, 272−279.

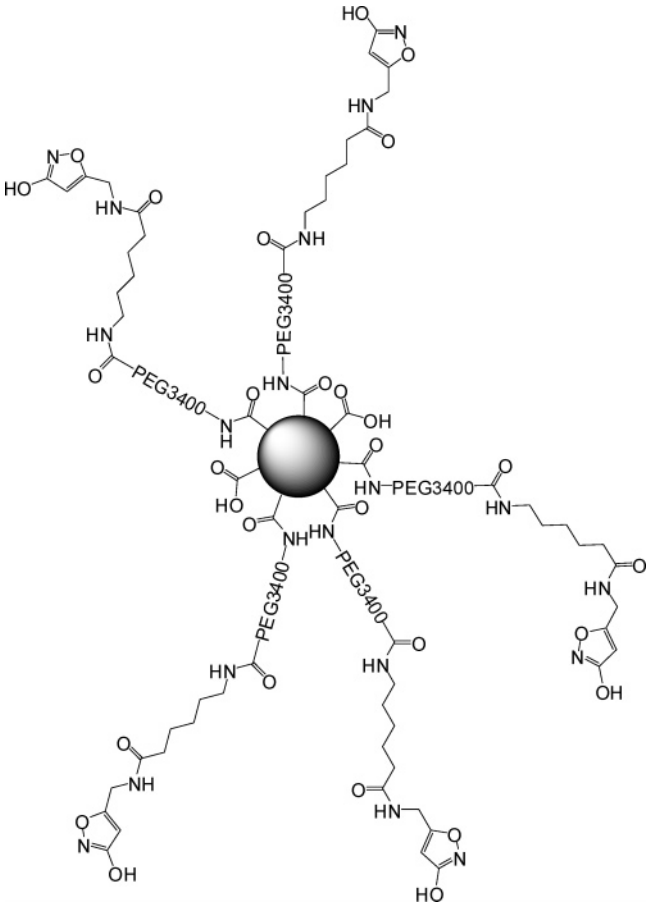

Figure 1. Structure of the investigated muscimol−PEG−qdot (M−PEG−qdot) preparation. The sphere represents the AMP-coated CdSe/ZnS qdot.

hydrochloride (EDC), after which the conjugate, henceforth referred to as M−PEG−qdot (muscimol−PEG−qdot), was purified by size exclusion chromatography (Sephadex G-50) and analyzed for concentration by absorbance spectrophotometry. We also prepared a qdot conjugate consisting of methyl-terminated PEG 2000 conjugated to qdots, i.e., a conjugate that lacked the terminating aminohexanoyl muscimol of the primary structure described in Figure 1. This preparation, henceforth referred to as PEG−qdots, was prepared using a Gabriel synthesis, as follows. Commercially obtained monomethoxy terminated PEG 2000 was converted to monoaminomethoxy terminated PEG 2000 by converting the terminal hydroxyl functionality to a tosylate (**5**). The tosylate was then displaced by refluxing it in acetonitrile with potassium phthalimide, yielding **6**. Finally, the phthalimide was converted to the amine **7** using hydrazine monohydrate. The following paragraphs describe details of the synthesis and analysis of structures **1**−**7** noted above.

C. {5-[(3-Hydroxyisoxazol-5-ylmethyl)carbamoyl]pentyl}carbamic Acid *tert*-Butyl Ester (1). Muscimol (0.1 g, 0.88 mmol) and 6-*tert*-butoxycarbonylaminohexanoic acid 2,5-dioxopyrrolidin-1-yl ester (0.29 g, 0.88 mmol) were dissolved in pyridine (5 mL), and the mixture was stirred at room temperature for 18 h. After evaporation, the product was purified via column chromatography on silica gel and eluted with methylene chloride (92%)/methanol (8%). The partially purified compound was further purified by washing with diethyl ether (10 × 10 mL). This yielded 0.15 g (54%) of the desired product as a colorless solid (melting point: 135−136 °C). ^{1}H NMR (acetone-d_6) 1.34−1.49 (m, 13H), 1.58−1.67 (m, 2H), 2.53 (t, 2H), 3.06 (q, 2H), 4.38 (d, 2H), 5.86 (s, 1H), 5.97 (s, 1H), 7.68 (s, 1H), 9.90 (brs, 1H).

D. 6-Aminohexanoic Acid [3-Hydroxyisoxazol-5-ylmethyl]amide (2). {5-[(3-Hydroxyisoxazol-5-ylmethyl)carbamoyl]pentyl}carbamic acid *tert*-butyl ester (0.2 g, 0.64 mmol) was dissolved in 95% TFA (2 mL) and stirred at room temperature for 1 h. The solution was evaporated and dried under reduced pressure for 4 days. The crude product was used without further purification. ^{1}H NMR (DMSO-d_6) 1.14−1.15 (m, 2H), 1.68−1.69 (m, 2H), 1.83−1.84 (m, 2H), 2.30−2.33 (m, 2H), 2.59 (s, 2H), 3.85 (s, 2H), 4.40 (d, 2H), 5.90 (s, 1H), 8.00 (s, 1H), 9.95 (s, 1H).

E. BOC-Protected Muscimol Derivative (3). 0.2 g of *tert*-butyloxycarbonyl (BOC) amine-PEG-activated acid (BOC-NH-PEG-NHS) was weighed out in a round-bottomed flask, and pyridine (2 mL) was added. 6-Aminohexanoic acid [3-hydroxyisoxazol-5-ylmethyl]-amide (0.04 g, 0.01 mmol) was dissolved in pyridine (1 mL) and added. The mixture was stirred at room temperature for 18 h and then evaporated under reduced pressure. The crude product was washed with diethyl ether (5 × 20 mL) and dried under reduced pressure. The resulting product was obtained as a brown tar. MALDI mass spectroscopy confirmed that the PEG had reacted with the 6-aminohexanoic acid [3-hydroxyisoxazol-5-ylmethyl]amide, and this product was used without further purification. ^{1}H NMR (acetone-d_6) 1.41−1.48 (m, 11H), 1.60−1.68 (m, 2H), 2.20−2.25 (m, 2H), 2.49 (t, 2H), 3.20−3.21 (m, 2H), 3.60 (nH), 4.40 (d, 2H), 5.91 (s, 1H), 5.95 (s, 1H), 8.01 (s, 1H).

F. Deprotected Muscimol (4). The BOC-protected muscimol compound was stirred in a mixture of 95% TFA (5 mL) and methylene chloride (5 mL) for 1 h, and the solvent was removed by evaporation under reduced pressure. The product was washed with diethyl ether (5 × 20 mL) and then dried under reduced pressure for 1 week. MALDI mass spectroscopy confirmed that the BOC group had been removed. After drying for 1 week, the product was obtained as a tar that was used without further purification.

G. Monomethoxy Tosyl PEG 2000 (5). PEG 2000 monomethyl ether (20 g) was dissolved in methylene chloride (200 mL) and cooled to 0 °C in an ice/acetone bath. *para*-Toluenesulfonyl chloride (2 g, 0.01 mol) was added, and the mixture was stirred at 0 °C for 30 min. Freshly powdered potassium hydroxide (4.5 g, 0.08 mol) was added, and the mixture was stirred at room temperature for 6 h. After warming to room temperature, the solution was washed with water (2 × 20 mL) and dried over magnesium sulfate. The methylene chloride was removed under reduced pressure, and the product was purified by washing with hexanes (5 × 200 mL). This yielded 18 g of the product as a waxy solid. ^{1}H NMR ($CDCl_3$) δ 2.42 (s, 3H), 3.39 (s, 3H), 3.60 (s, nH), 3.82−3.86 (m, 2H), 4.10−4.14 (m, 2H), 7.31 (d, 2ArH), 7.75 (d, 2ArH).

H. Monophthalimido PEG 2000 Monomethyl Ether (6). Monotosyl PEG 2000 monomethyl ether (18 g) and potassium phthalimide (1.31 g) were dissolved in acetonitrile (200 mL) and heated at reflux with stirring for 18 h. The mixture was cooled, evaporated, and dissolved in methylene chloride (200 mL). The organic solution was washed with water (2 × 50 mL) and dried over magnesium sulfate. After filtering and evaporating under reduced pressure, the crude product was purified by washing with hexanes (5 × 200 mL). This yielded 7.7 g of the product (**6**) as a colorless wax. ^{1}H NMR ($CDCl_3$) δ 3.36 (s, 3H), 3.52 (s, nH), 3.68 (m, 2H), 3.82 (m, 2H), 7.69 (m, 2ArH), 7.79 (m, 2ArH).

I. Monoamino PEG 2000 Monomethyl Ether (7). Monophthalimido PEG 2000 monomethyl ether (7.7 g) was dissolved in ethanol (200 mL), and hydrazine monohydrate (10 mL) was added. The mixture was stirred at room temperature for 18 h and then evaporated under reduced pressure. The crude product was dissolved in methylene chloride and stirred for 18 h at room temperature. The solution was filtered and washed with water (2 × 50 mL) and dried over magnesium sulfate. After filtration and evaporation, the product was purified by washing with hexanes (5 × 200 mL). This yielded the product (**7**) as a colorless wax (5.9 g). ^{1}H NMR ($CDCl_3$) δ 3.32 (s, 3H), 3.56 (s, nH), 3.69 (m, 2H).

J. Derivatization of qdots with Structures 4 and 7. 1. Muscimol-Containing Structure (4). 0.1 mL of an 8.4 μM solution of qdots was placed in a vial equipped with a stir bar. To this was added 0.3 mL of borate buffer (pH 8.5) that contained 3 mg (1000 equiv) of the

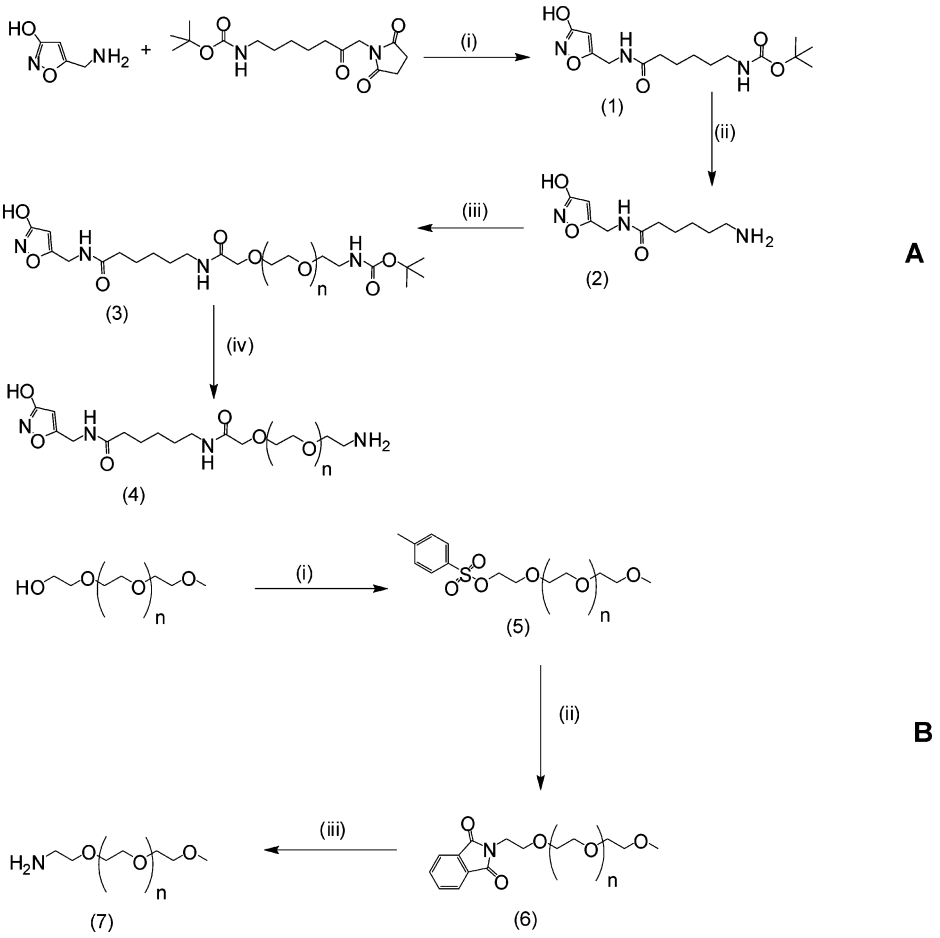

Figure 2. Synthetic schemes for compounds that were conjugated to qdots. (A) Route used for synthesis of muscimol-containing compound **4**. (i) Pyridine, room temperature, 18 h; (ii) trifluoroacetic acid, room temperature, 1 h; (iii) *tert*-butoxycarbonylamine-PEG-activated acid, pyridine, room temperature, 18 h; (iv) trifluoroacetic acid, methylene chloride, room temperature, 1 h. Here and in panel B, the value of the subscript *n* (denoting the number of ethylene glycol units in PEG 3400) is ~78. (B) Route for synthesis of compound **7**. (i) Potassium hydroxide, *para*-toluenesulfonyl chloride, methylene chloride, 0 °C, 6 h; (ii) potassium phthalimide, acetonitrile, reflux, 18 h; (iii) (a) ethanol, hydrazine hydrate, room temperature, 18 h; (b) methylene chloride, room temperature, 18 h.

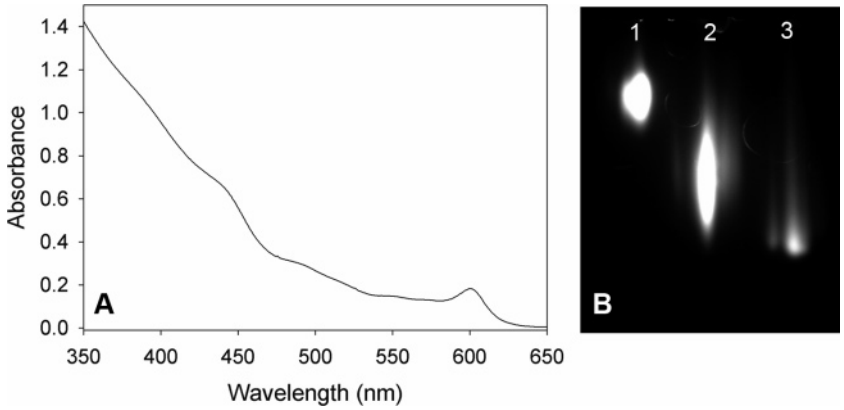

Figure 3. (A) UV−visible spectrum of M−PEG−qdots. (B) Agarose gel electrophoresis (1% agarose gel, TAE buffer; 80 mV potential difference) of AMP-coated qdots vs muscimol-conjugated qdots. Lane 1: PEG2000−qdots. Lane 2: M−PEG−qdots. Lane 3: AMP-coated qdots.

muscimol-containing compound (**4**). Then *N*-hydroxy succinimide (72 μg, 0.63 μmol) dissolved in borate buffer (0.1 mL) was added. This was followed by the addition of 1-[3-(dimethylamino)propyl]-3-ethylcarbodiimide hydrochloride (EDC) (0.12 mg, 0.63 μmol) dissolved in borate buffer (0.1 mL). The mixture was stirred at room temperature for 2 h, then purified by passage through a Sephadex G-50 column, and eluted with borate buffer (pH 8.5). The fluorescent fractions were combined to yield the purified muscimol-functionalized qdots (M−PEG−qdots). Figure 3A shows a UV−visible spectrum of the M−PEG−qdots. The spectrum is dominated by the absorbance of the qdot itself, exhibiting a peak near 600 nm indicative of the first excited state. The absorbance continuously increases at shorter wavelengths due to excitation of higher-lying electronic states. This spectral line shape is typical for quantum dots. The spectrum blue-shifts for smaller dots and red-shifts for larger dots owing to "particle-in-a-box" quantum mechanical properties.[45] The concentration of qdots in this preparation was determined based on a molar extinction coefficient of 6.5×10^5 M^{-1} cm^{-1} at 600 nm (private communication, M. Bruchez). The

derivatization of qdots with the muscimol- and PEG 3400-containing structure (**4**) and with the PEG 2000-containing structure (**7**) that lacked muscimol was evaluated by electrophoresis in 1% agarose gels using Tris-acetate-EDTA (TAE) buffer, pH 7.4 (Figure 3B). Underivatized AMP-coated qdots were used as a control. The evident streaking of the M−PEG−qdot conjugate is attributed to variability in loading of the qdots with the muscimol-containing structure. Agarose gel electrophoresis of qdots derivatized with the PEG 2000-containing structure (**7**) also showed that these qdots were functionalized. The coupling efficiency for the conjugation of structure **7** to AMP qdots has previously been observed to be ∼20%.[29] As the present muscimol-containing M−PEG−qdot (Figure 1) is a derivative of PEG 3400, a similar coupling efficiency is likely. Hence, each qdot of the M−PEG−qdot was presumed to be derivatized with approximately 150−200 muscimol groups on average. Conjugation was attempted using a much higher (2000-fold) molar excess of the muscimol-containing structure, but this higher loading condition led to precipitation of the conjugates. Qdots conjugated with 1000 equiv and 2000 equiv of the muscimol ligand were imaged using an inverted microscope. These images clearly show that the qdots had formed a precipitate when 2000 equiv were used. However, when 1000 equiv were used, no precipitation was observed (see Supporting Information). We attribute this precipitation observed with high loading as due either to increased lipophilicity of the resulting conjugate or to the formation of multiple hydrogen bonds between muscimol groups on different qdots. In addition to precipitation, higher loading with the muscimol-containing structure led to a significant quenching of qdot fluorescence. Such a quenching phenomenon has previously been observed[29] and attributed to the ratios of EDC and NHS used for preparation of the conjugate. Quantum yields were measured for the unconjugated AMP-coated qdots and qdots conjugated with 1000 equiv of muscimol ligand and found to be 0.297 and 0.137, respectively, for these materials (see Supporting Information). Both the AMP-coated qdots and the muscimol conjugates showed robust fluorescence and exhibited little photobleaching over a time course of 1 h (Supporting Information).

2. Monoamino Monomethyl Ether (7). 0.1 mL of a solution containing 2000 equiv of **7** in borate buffer at pH 8.5 was placed in a reaction vial equipped with a magnetic stirrer. To this was added 0.1 mL of a borate solution containing 1500 equiv of NHS, 0.1 mL of an 8.5 μM solution of qdots in borate buffer, and 0.1 mL of a solution containing 1500 equiv of EDC in borate buffer. This mixture was stirred for 2 h at room temperature, and the PEGylated qdots were purified by size exclusion chromatography on Sephadex G-50, yielding the conjugate PEG 2000 with the qdots (PEG−qdots). The concentration of the qdot preparation was determined by UV−visible spectroscopy, using an extinction coefficient of 6.5×10^5 M^{-1} cm^{-1}. By analogy with the considerations noted above for the M−PEG−qdot preparation, we estimate that average loading in the PEG−qdot preparation was ∼300−400 PEG 2000s per qdot.

K. MALDI TOF Mass Spectroscopy. Compounds **3** and **4** were characterized using MALDI TOF mass spectroscopy. MALDI-TOF mass spectra were recorded on an Applied Biosystems Voyager mass spectrometer equipped with a 337 nm nitrogen laser. The acceleration voltage was 25 kV, and 30 to 64 scans were averaged for each spectrum. For sample preparation, a saturated matrix stock solution of 2,5-dihydroxybenzoic acid and a 0.01 M sodium iodide solution were prepared in methanol. Stock solutions of poly(ethylene glycol) amine (5 mM) in methanol and the poly(ethylene glycol) conjugates in water were prepared. The stock solutions were mixed in a 2:5:2 ratio of sample-to-matrix-to-salt by volume. A 1 μL aliquot of each sample solution was placed on the sample plate. A PEG standard prepared in the same manner as the other samples was used for mass calibration of the instrument. The resulting spectra indicated that compounds **3** and **4** were polydisperse. Compound **3** exhibited masses ranging from 3241 to 4188 Da, indicating the conjugation of muscimol to PEGs of different lengths. The peak of greatest intensity had a mass of 3726 Da. When compound **3** was treated with TFA to yield compound **4**, the observed masses in the MALDI TOF spectrum shifted by 100 Da, corresponding to loss of the BOC protecting group, and the most intense peak was observed to have a mass of 2626 Da. In addition, a MALDI TOF mass spectrum obtained for compound **7** was found to be consistent with the desired structure.

Oocyte Preparation and Receptor Expression. All animal procedures adhered to institutional policies and to the Statement for the Use of Animals in Ophthalmic and Vision Research adopted by the Association for Research in Vision and Ophthalmology (ARVO). Ovarian lobes of gravid adult female *Xenopus laevis* toads (Xenopus One, Ann Arbor, MI), anaesthetized with MS-222 (1 g/L), were excised, and the oocytes were removed. Stages V−VI oocytes were selected and stored in frog Ringer solution (100 mM NaCl, 2 mM KCl, 2 mM $CaCl_2$, 1 mM $MgCl_2$, 10 mM glucose, and 5 mM HEPES, pH 7.4). The follicular layer was removed by 30 min-immersion of the oocytes in Ca^{2+}-free Ringer solution containing 2 mg/mL collagenase, at room temperature. The expression of $GABA_C$ receptors (human ρ1 and perch ρ1B) in *Xenopus laevis* oocytes was achieved using previously described procedures.[40,46] cRNA (50 nL), obtained for each $GABA_C$ receptor subunit from in vitro transcription (mMessage mMachine Ambion Inc., Austin, TX) from linearized cDNAs, was injected into the oocytes (Drummond Nanoject II; Drummond Scientific Co., Broomall, PA). Oocytes were assayed after 18−72 h storage in Ringer solution containing 0.1 mg/mL gentamycin at 16−19 °C, to allow for expression of the $GABA_C$ receptors. Control oocytes were obtained either by leaving the oocytes uninjected or by injecting water only rather than cRNA solution.

Confocal Microscopy. Images were obtained from oocytes positioned in a glass-bottom dish and incubated for defined periods in Ringer solution supplemented with one or more test components. Experiments were conducted at ambient temperature (range: 16−20 °C). To prevent degradation of the oocyte, the maximum duration of an experiment was 60 min. After each incubation or washing step, the oocytes were visually inspected to detect evidence of membrane disruption and discarded if such occurred. Below we will use the terms one-, two-, and three- phase incubations to denote the conditions of treatment of the oocytes. *One-phase incubation*: Oocytes were bathed in a drop of 34 nM M−PEG−qdot in Ringer solution for 5−10 min and imaged. *Two-phase incubation*: To determine the binding of M−PEG−qdots in the presence of putative competitors, we conducted experiments that involved initial incubation with the test competitor, followed by incubation in the presence of both test competitor and M−PEG−qdots. The test competitors investigated were the following: GABA (100 μM to 5 mM); free muscimol (100 μM to 5 mM); unconjugated qdots (34 nM); a conjugate consisting of PEG 3400 joined to muscimol ("PEG−muscimol") (500 μM); and a conjugate that consisted of PEG 2000 joined to qdots ("PEG−qdots") (34 nM). The first phase of each experiment involved 15-min incubation with the test competitor at a defined concentration. At the conclusion of this first-phase incubation, and after collection of an initial image when the test competitor was itself fluorescent (unconjugated qdots or PEG−qdots), the oocyte was removed from the surrounding medium, transferred to a drop (∼35 μL) of medium that contained the test competitor (at a concentration identical to that of the first incubation) along with 34 nM M−PEG−qdots, and maintained for 15 min in this latter medium (second-phase incubation). The oocyte was imaged at the conclusion of this second incubation. *Three-phase incubation*: Immediately following the two-phase protocol just described, the oocyte was removed from the medium containing GABA (100 μM−5 mM) plus 34 nM M−PEG−qdot, washed twice in Ringer for 5 min each, then incubated for 5−10 min

(45) Kippeny, T.; Swafford, L. A.; Rosenthal, S. J. *J. Chem. Ed.* **2002**, *79*, 1094−1100.

(46) Vu, T. Q.; Chowdhury, S.; Muni, N. J.; Qian, H.; Standaert, R. F.; Pepperberg, D. R. *Biomaterials* **2005**, *26*, 1895−1903.

in 34 nM M−PEG−qdot alone (third-phase incubation), and then immediately imaged.

Fluorescence was measured using a confocal microscope (Leica model DM-IRE2 with 20× objective) with excitation at 476 nm. Fluorescence emission was detected over a wavelength interval (580−620 nm) that included the qdot emission peak (λ = 605 nm). Microscope settings relevant to excitation illumination and detection of fluorescence emission (gain and offset) were established at the beginning of experiments conducted on a given day, using either a human ρ1- or perch ρ1B-expressing oocyte bathed in 34 nM M−PEG−qdot, and maintained without change for the entire day's measurements. For optical clarity of both the fluorescence and bright-field images obtained from the (opaque) oocyte, the microscope was focused on the oocyte's equatorial plane. In all experiments, the pinhole was maintained at one airy unit to maximize resolution. On a given day, each set of experiments was performed on a single batch of oocytes and employed a single preparation of M−PEG−qdot in Ringer solution. Experiments involving single-phase incubations were conducted both on oocytes expressing human ρ1 and oocytes expressing perch ρ1B $GABA_C$ receptors; most two- and three-phase protocols were performed on oocytes expressing human ρ1 $GABA_C$ receptors.

Image Analysis. Each fluorescence image was analyzed using MetaMorph Offline version 6.3r0 software (Universal Imaging Corp., Downingtown, PA), as follows. *Oocyte surface membrane*: Under visual control, the cursor was used to trace the arclike border of the oocyte as a series of 15−25 straight-line segments that spanned the entire field of view of the border and included 450−750 pixels (i.e., data points). The cumulative length of this multisegmented line was noted. Tabulated data for the "Border" region (see Results) indicate fluorescence intensity values for the pixels covered by this multisegment line. *Surrounding medium*: Fluorescence of the medium bathing the oocyte was taken as a background to which the oocyte border fluorescence was referred. For determination of background fluorescence, the multisegment line used to determine the border fluorescence was copied and replicated to cover a representative region in the medium (mean translation distance: 46 μm; range: 34−75 μm); the intensities of pixels covered by this segmented line were then obtained (tabulated data for the "Background" region in the Results). *Oocyte interior*: The fluorescence of the oocyte interior was in all cases comparable to or less than that of the external region and was not quantitatively analyzed.

The assessment of fluorescence intensity differences both within and between images required consideration of sample-to-sample variability for both the border and background characterization. To account for this variability we conducted analyses of variance (ANOVA). This type of analysis allows for the evaluation of differential changes across images when, for example, the background intensities fluctuate. In addition, due to the punctate nature of the fluorescence, i.e., to the presence of "hot spots" of high fluorescence intensity, we anticipated the occurrence of non-normal distributions of pixel intensities across an image. To evaluate the distribution of signal intensities both within border and background regions of a given image and between borders and backgrounds across images we assessed the shape of the fluorescence intensity distributions using chi-square (χ^2), a nonparametric test. In those cases for which there was a significant shift in the shape of the distribution, we have included the appropriate χ^2 statistics in the text. Throughout the Results text, differences in image intensities are evaluated by means of ANOVA, and differences or shifts in the distribution of signal intensities are characterized by χ^2. Because of the large sample size analyzed (450−750 pixel values per image), most comparison analyses yielded results with extremely low values ($p < 10^{-6}$), regardless of the differences between mean values. Accordingly, to evaluate the significance of the similarities or differences in data sets being compared, we determined values of eta-square (η^2), a parameter that characterizes the magnitude of the differences for each statistical comparison.[47] The value of η^2 ranges from 0 to 1, with $\eta^2 \leq 0.01$ conventionally classified as small, $\eta^2 \leq 0.06$ as moderate, and $\eta^2 \geq 0.14$ as large.[47,48]

Results

Binding of M−PEG−qdots. To assess the interaction between the synthesized M−PEG−qdot and $GABA_C$ receptors, we tested whether we could visualize binding of the fluorescent compound at the surface of oocytes expressing either human ρ1 or perch ρ1B $GABA_C$ receptors. Figure 4 shows results obtained with a one-phase incubation from $GABA_C$-expressing and control oocytes. Figure 4A shows results obtained with incubation of a human ρ1-expressing oocyte in the presence of 34 nM M−PEG−qdots. Here the fluorescence image of the oocyte was obtained after 5-min incubation in the M−PEG−qdot-containing medium. The image shows a thin halo of fluorescence at the oocyte surface, the intensity of which exceeded the surround fluorescence. The fluorescence image may be compared with the simultaneously obtained bright-field image, which illustrates the position and focus of the oocyte. A relatively sharp halo of fluorescence was observed with a perch ρ1B-expressing oocyte similarly treated with M−PEG−qdots in a single-phase incubation (Figure 4B). Within a given group, results obtained with oocytes expressing either human ρ1 or perch ρ1B $GABA_C$ receptors, and incubated in the presence of M−PEG−qdots only, were taken as the positive control. By contrast with the results shown in panels A−B, only diffuse surround fluorescence was observed when an untreated (i.e., noninjected) oocyte that presumably lacked $GABA_C$ receptors was incubated with M−PEG−qdots (Figure 4C). Similarly, only diffuse surround fluorescence was observed with oocytes that received an injection of water rather than cRNA solution (not illustrated). Because diluting the M−PEG−qdot preparation in borate buffer into Ringer yields a solution with a pH of about 7.9, we assessed whether the elevated pH played a role in the binding, by lowering the pH of a 34 nM PEG−M−qdot solution to 7.2 with HCl and testing its binding to $GABA_C$-expressing and -nonexpressing oocytes. Under these conditions, a fluorescence halo was observed for all tested $GABA_C$-expressing oocytes (n = 4) but not for nonexpressing oocytes (n = 3) (data not shown).

The border of the oocyte described by Figure 4A was analyzed for fluorescence intensity (see Experimental Section). For the human ρ1-expressing oocyte, this analysis yielded 67.31 ± 36.79, as shown by the "border" entry in Table 1, row 1. By comparison, fluorescence analysis of a representative multisegment line in the surround medium, henceforth termed the background fluorescence, exhibited a significantly lower fluorescence intensity of 22.30 ± 21.18 (row 1, "background") (ANOVA: $F(1, 580) = 696.26$, $p < 10^{-6}$, $\eta^2 = 0.54$). Border and background data obtained from the perch ρ1B-expressing oocyte of Figure 4B similarly exhibited a large border vs background difference and large SDs (Table 1, row 2) ($F(1, 479) = 814.51$, $p < 10^{-6}$, $\eta^2 = 0.63$). For the nonexpressing oocyte of Figure 4C, the fluorescence intensity of the border did not exceed that of the background (Table 1, row 3). Furthermore, two-way ANOVA showed that the relationship between border and background intensity depended on receptor

(47) Cohen, J. *Statistical power analysis for the behavioral sciences*; Lawrence Erlbaum Associates, Inc.: Hillsdale, NJ, 1977.
(48) Stevens, J. *Applied Multivariate Statistics for the Social Sciences*, 3rd ed.; Erlbaum: Hillsdale, NJ, 1996; p 177.

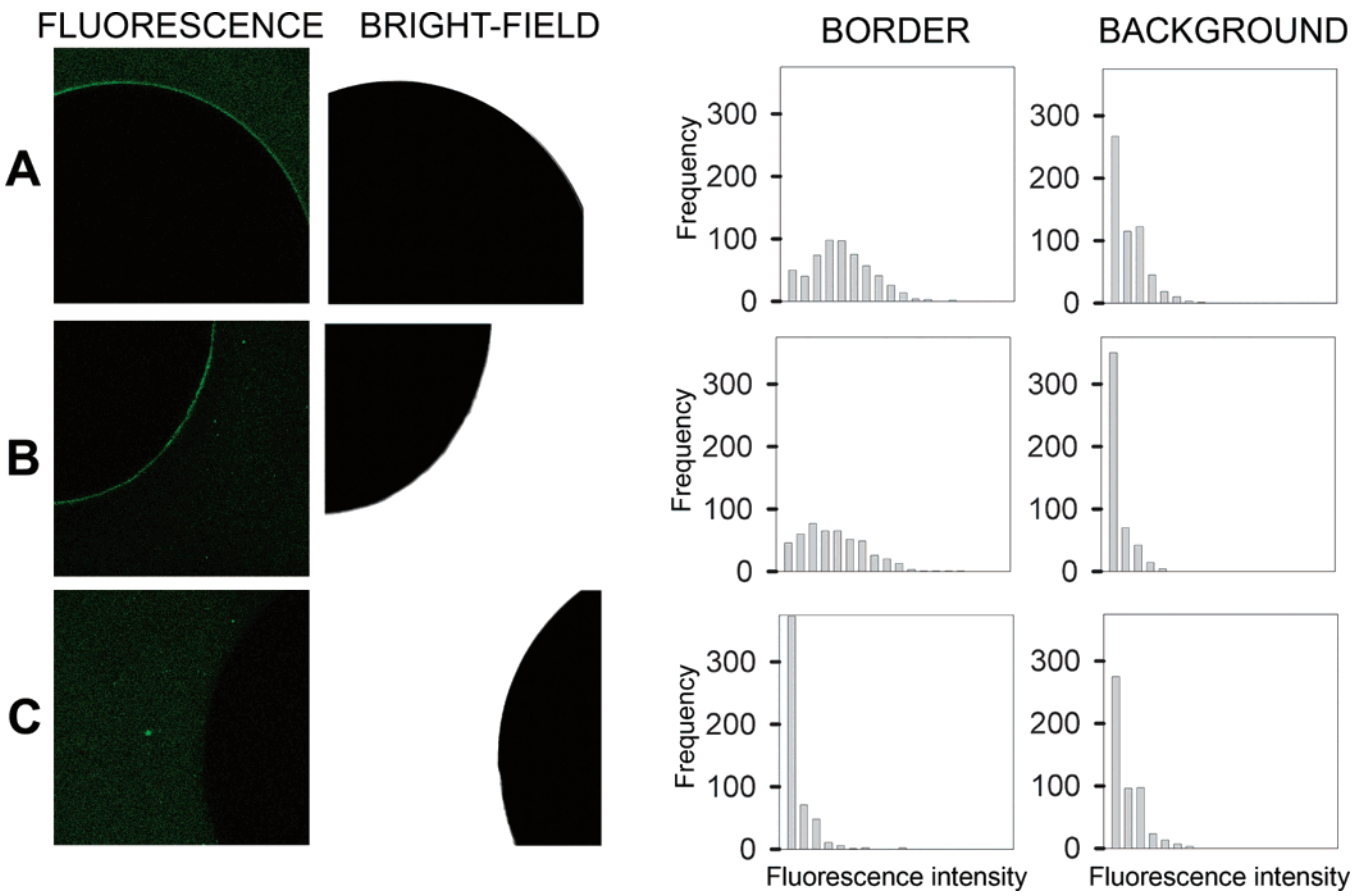

Figure 4. Representative single-phase experiments involving incubation of the oocyte with 34 nM M−PEG−qdots. (A−B) Results obtained with oocytes expressing human ρ1 (A) and perch ρ1B (B) $GABA_C$ receptors. (C) Results obtained with a noninjected oocyte. Within each panel (i.e., within each row of the figure) are shown a fluorescence image obtained from a single representative oocyte after a 10-min incubation with the M−PEG−qdots and the corresponding bright-field image of the (opaque) oocyte in the plane of focus. Each panel also indicates the distributions of fluorescence intensity for the border and background regions determined from the illustrated fluorescence image. Here and in subsequent figures, distributions of border and background intensities are plotted with fixed bin widths, each spanning 15 gray scale units.

expression, specifically showing a significant difference in border vs background intensity for ρ1- and ρ1B-expressing oocytes but not for nonexpressing oocytes ($F(2, 1572) = 411.79$, $p < 10^{-6}$, $\eta^2 = 0.34$; where border and background measures are within-sample comparisons and ρ1, ρ1B, and nonexpressing oocytes are between-sample comparisons). We interpret the relatively large SDs of the border data for the ρ1- and ρ1B-expressing oocytes to be due to nonhomogeneous coverage of the oocyte surface membrane by the M−PEG−qdot (due, presumably, to nonuniform expression and/or clustering of GABA receptors on the cell membrane). The large SDs for the background data, and for the border data obtained from the nonexpressing oocyte, are interpreted as due to the punctuate nature of surround fluorescence of the qdot suspension, together with a possible aggregation of the M−PEG−qdots. Further insight into the characteristics of fluorescence properties described by rows 1−3 in Table 1 comes from considering the distribution of fluorescence intensity of the pixels themselves. Information on the shapes of these distributions is shown by the histograms of Figure 4, which illustrate distributions of pixels for the border and background regions of the corresponding Figure 4 fluorescence image.

Rows 4−6 of Table 1 show aggregate results obtained for border and background fluorescence among groups of oocytes. These data were obtained from measurements conducted on multiple replicates (human ρ1 positive control: $n = 11$; perch ρ1B positive control: $n = 4$; negative control: $n = 14$) on different experiment days. Comparison by two-way mixed-design ANOVA of the border versus background fluorescence for the human ρ1- and perch ρ1B-expressing oocytes, relative to nonexpressing oocytes, indicated a significant difference in fluorescence intensity ($F(2, 15\,507) = 4285.13$, $p < 10^{-6}$, $\eta^2 = 0.37$). Specifically, the respective values for border and background regions were 88.84 ± 64.84 and 31.60 ± 35.50 for human ρ1-expressing oocytes; 109.58 ± 58.42 and 18.54 ± 16.47 for perch ρ1B-expressing oocytes; and 15.14 ± 22.35 and 16.78 ± 22.17 for nonexpressing oocytes. This two-way ANOVA demonstrates a significant difference between border and background intensities for both the human ρ1 and perch ρ1B, whereas there is no difference between border and background intensities for the nonexpressing oocytes. Near-maximum fluorescence intensity was typically reached early in the period of incubation. That is, fluorescence intensities measured after 2−3 and 5 min of exposure of $GABA_C$-expressing oocytes to M−PEG−qdots (data not shown) were comparable with intensities measured after 10-min incubation (Figures 4 and 5, and Table 1).

For the aggregate data obtained from multiple replicates (groups identified above), there was a significant difference in both the intensity and the shape of the distribution of values for border relative to background for human ρ1-expressing oocytes ($F(1, 6376) = 6050.72$, $p < 10^{-6}$, $\eta^2 = 0.49$;

Table 1. Fluorescence Intensities of Oocyte Surface Membrane (Border) and Surrounding Regions (Background)

row	figure	$GABA_C$ receptor	test agent(s)	border[a] (mean ± SD)	background[a] (mean ± SD)
1	Figure 4A	ρ1	M−PEG−qdot	67.31 ± 36.79	22.30 ± 21.18
2	Figure 4B	ρ1B	M−PEG−qdot	62.34 ± 38.56	9.65 ± 14.67
3	Figure 4C	nonexpressing	M−PEG−qdot	10.16 ± 18.17	18.56 ± 19.95
4		ρ1	M−PEG−qdot (n = 11)[b]	88.84 ± 64.84	31.60 ± 35.50
5		ρ1B	M−PEG−qdot (n = 4)[b]	109.58 ± 58.42	18.54 ± 16.47
6		nonexpressing	M−PEG−qdot (n = 14)[b]	15.14 ± 22.35	16.78 ± 22.17
7	Figure 7B	ρ1	(1) GABA (100 μM), (2) M−PEG−qdot plus 100 μM GABA	16.10 ± 25.54	4.58 ± 8.91
8	Figure 7C	ρ1	(1) Muscimol (100 μM), (2) M−PEG−qdot plus 100 μM muscimol	12.16 ± 17.47	3.69 ± 8.31
9	Figure 7D	ρ1	(1) M−PEG (500 μM), (2) M−PEG−qdot plus 500 μM M−PEG	32.05 ± 31.26	4.91 ± 10.27
10	Figure 8B	ρ1[c]	unconjugated qdot (34 nM)	16.29 ± 24.19	13.21 ± 18.16
11	Figure 8C	same ρ1 (10)[c]	(1) unconjugated qdot (34 nM), (2) M−PEG−qdot (34 nM) plus 34 nM unconjugated qdot	89.94 ± 58.07	30.71 ± 23.54
12	Figure 8D	ρ1[C]	PEG−qdot (34 nM)	1.52 ± 5.77	1.80 ± 6.39
13	Figure 8E	same ρ1 (12)[c]	(1) PEG−qdot (34 nM), (2) M−PEG−qdot (34 nM) plus 34 nM PEG−qdot	140.10 ± 86.82	18.02 ± 21.11
14	Figure 9B	ρ1[c]	(1) GABA (100 μM), (2) M−PEG−qdot plus 100 μM GABA	22.41 ± 32.71	7.32 ± 12.30
15	Figure 9C	same ρ1 (14)[c]	(1) GABA (100 μM), (2) M−PEG−qdot plus 100 μM GABA, (3) wash, and M−PEG−qdot (34 nM)	119.51 ± 84.47	11.83 ± 15.01

[a] Data indicated in the border and background columns of each row are the means ± SDs of fluorescence intensities determined with a 0−255 gray scale. [b] Results shown in rows 4−6 are aggregate data determined in the indicated number of experiments. For all other rows, the data indicate results obtained in a single experiment; each of these experiments is illustrated as denoted in the "figure" column. [c] Data indicated in rows 11, 13, and 15 were obtained from the same oocytes as those described in rows 10, 12, and 14, respectively.

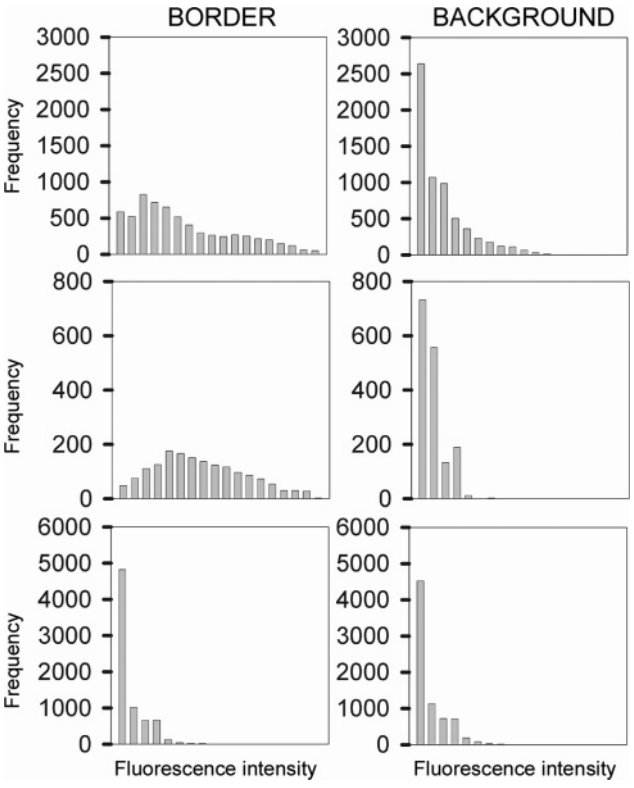

Figure 5. Aggregate data for distributions of border and background intensity obtained in single-phase experiments on human ρ1-expressing oocytes (A) (n = 11), perch ρ1B-expressing oocytes (B) (n = 4), and nonexpressing oocytes (C) (n = 14).

$\chi^2(11\,929) = 12\,567.6$, $p = 2.4 \times 10^{-5}$). Similarly, for perch ρ1B-expressing oocytes, there was a significant difference in both shape (Figure 5) and intensity of the distribution for border vs background regions ($F(1, 1685) = 4028.97$, $p < 10^{-6}$, $\eta^2 = 0.71$; $\chi^2(7420) = 7751.8$, $p = 0.004$). Border vs background data obtained from nonexpressing oocytes also showed a significant difference in the distribution of intensity values but, by contrast with the results obtained from human ρ and perch ρ1B-expressing oocytes, showed no difference in distribution shape ($F(1, 7446) = 27.93$, $p < 10^{-6}$, $\eta^2 = 0.004$; χ^2 (3944) = 4086.5, $p = 0.056$).

The removal of M−PEG−qdots from $GABA_C$-expressing oocytes was investigated in wash-out experiments. Following treatment for 5−10 min with 34 nM M−PEG−qdots, the oocyte was immersed for 2−5 s in a ligand-free medium and then transferred to a static bath of ligand-free medium (Ringer solution) for further incubation. Figure 6 shows results obtained in experiments of this type on human ρ1 and perch ρ1B $GABA_C$ receptor-expressing oocytes. In each experiment, normalized fluorescence intensity F/F_0 of the border region was determined at the conclusion of the incubation with M−PEG−qdots (t = 0) and defined times following transfer of the oocyte into the initially ligand-free medium. The data obtained from human ρ1 and perch ρ1B $GABA_C$ receptor-expressing oocytes indicated that a 50% decrease in normalized fluorescence intensity required incubation for roughly 10−15 min in this latter medium.

Competition with M−PEG−qdot Binding. A. Two-Phase Incubations. To test whether known $GABA_C$ agonists and other test agents can compete with M−PEG−qdot for binding, we conducted experiments involving two-phase incubation of the oocyte. In the first of these two phases, the oocyte was bathed for 15−20 min in a medium containing the test agent at a

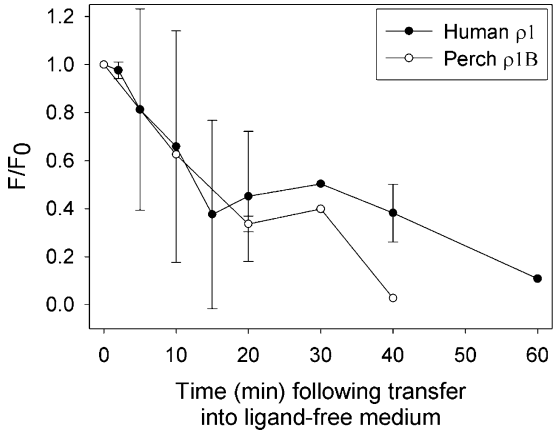

Figure 6. Wash-out of M−PEG−qdots from the border region of human ρ1-expressing and perch ρ1B-expressing oocytes ($n = 4$ and $n = 2$, respectively). In each experiment, fluorescence intensity of the border and background regions was determined following incubation with 34 nM M−PEG−qdots, rapid washing, and subsequent transfer into a ligand-free medium (see text). The net difference in fluorescence intensity (border minus background) obtained at a given time was normalized to that obtained at the conclusion of incubation with the M−PEG−qdots, to yield the normalized fluorescence intensity F/F_0. Filled circles show data obtained from human ρ1-expressing oocytes (1−4 determinations) as a function of time following transfer of the oocyte into the ligand-free medium. For multiple determinations, the data indicate the mean ± SD. Open circles show data obtained from perch ρ1B-expressing oocytes (1−2 determinations).

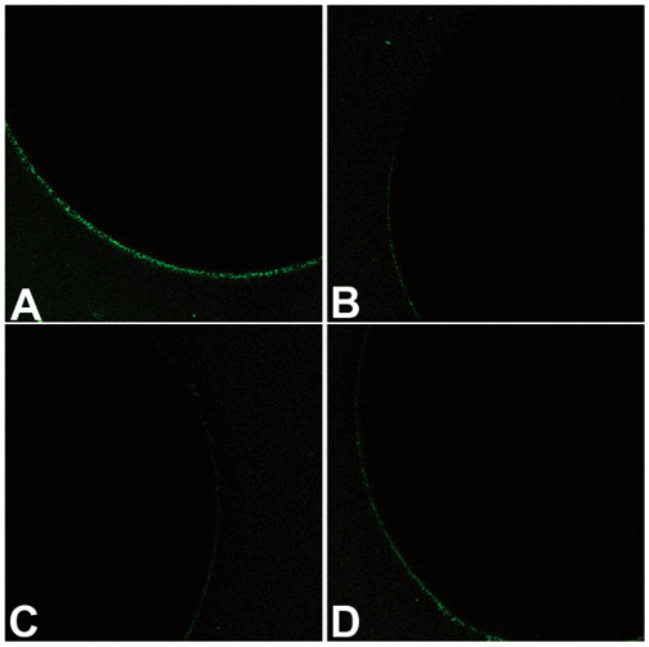

Figure 7. Two-phase experiments in oocytes expressing human ρ1 $GABA_C$ receptors. (A) Positive control for this series of observations (oocyte expressing human ρ1, imaged after a 5-min incubation in 34 nM M−PEG−qdots). (B) Two-phase incubation involving (1) 100 μM GABA and (2) 34 nM M−PEG−qdots in buffer supplemented with 100 μM GABA. (C) Two-phase incubation involving (1) 100 μM muscimol and (2) 34 nM M−PEG−qdots in buffer supplemented with 100 μM muscimol. (D) Two-phase incubation involving (1) 500 μM PEG−M and (2) 34 nM M−PEG−qdots in buffer supplemented with 500 μM PEG−M.

defined concentration. At the conclusion of this first "pretreatment" incubation period, the oocyte was immediately transferred to a medium containing both the same concentration of test agent and 34 nM M−PEG−qdots and further incubated for 10−15 min. The fluorescence image obtained at the conclusion of this second incubation was analyzed in relation to the image obtained from a positive control oocyte incubated only with 34 nM m−PEG−qdots. Figure 7A−B show, respectively, results obtained from a positive control oocyte (A) and those obtained from an oocyte subjected to 100 μM GABA treatment through the two-phase protocol just described (B). By comparison with the image obtained from the positive control, that obtained with 100 μM GABA as a test agent exhibited relatively little border fluorescence. The border intensity of this GABA-treated oocyte (Table 1, row 7) was significantly lower than that of the positive control run on the same experiment day (83.34 ± 64.82, not shown in Table 1), and the border distribution was significantly shifted from that of the control ($F(1, 1067) = 485.26$, $p < 10^{-6}$, $\eta^2 = 0.31$; $\chi^2(16\,770) = 17\,217.67$, $p = 0.008$). Two-phase incubation with either 500 μM GABA or 5 mM GABA also significantly reduced border intensity (for 500 μM GABA, $F(1, 1123) = 784.54$, $p < 10^{-6}$, $\eta^2 = 0.41$; and for 5 mM GABA, $F(1, 1052) = 639.06$, $p < 10^{-6}$, $\eta^2 = 0.38$). Furthermore, significant reductions in border intensity and shifts in distribution shape were produced by two-phase treatment with 100 μM (Figure 7C; Table 1, row 8), 500 μM, and 5 mM muscimol (data obtained under the latter two conditions not illustrated). Specifically, for 100 μM muscimol, $F(1, 1057) = 573.95$, $p < 10^{-6}$, $\eta^2 = 0.35$; $\chi^2(13\,056)\ 13\,375.85$, $p = 0.025$; for 500 μM muscimol, $F(1, 1235) = 922.75$, $p < 10^{-6}$, $\eta^2 = 0.43$; and for 5 mM muscimol, $F(1, 1158) = 843.37$, $p < 10^{-6}$, $\eta^2 = 0.42$. In addition, two-phase incubation with 500 μM M−PEG, a structure lacking the qdot, significantly reduced the border intensity (Figure 7D; Table 1, row 9) ($F(1, 1157) = 733.77$, $p < 10^{-6}$, $\eta^2 = 0.39$).

Two-phase experiments also were conducted with two qdot-based (and thus, fluorescent) structures in which the muscimol moiety was absent. In these experiments, images were obtained at the end of the first-phase incubation (treatment with the test competitor alone) as well as at the end of the second-phase incubation with both test competitor and 34 nM M−PEG−qdots. Figure 8A shows results obtained from the positive control preparation (human ρ1-expressing oocyte incubated with 34 nM M−PEG−qdots) investigated on the experiment day under consideration. Figure 8B−C and Table 1, rows 10−11 show results obtained from a human ρ1 $GABA_C$-expressing oocyte treated with unconjugated qdots (a structure lacking both poly(ethylene glycol) and muscimol) during the two phases of incubation. To compare the post-first-phase image (which itself exhibited fluorescence; Figure 8B and Table 1, row 10) and post-second phase image (Figure 8C and Table 1, row 11), we used two-way ANOVA with border and background measurements for within-sample comparison and the incubation phase for between-sample comparison. This allowed evaluation not only of the relationship between post-first-phase and post-second-phase border intensity but also of the ratio of border vs background intensity across the two incubation phases. The results ($F(1, 1142) = 377.85$, $p < 10^{-6}$, $\eta^2 = 0.25$) indicated that the change in border intensity between postphase 1 (15.79 ± 23.18) and postphase 2 (89.31 ± 58.62) was significant (as was the change in background intensity between postphase 1 and postphase 2; 13.13 ± 18.17 and 39.99 ± 23.80, respectively). The ratio of border-to-background intensity also increased significantly between postphase 1 and postphase 2.

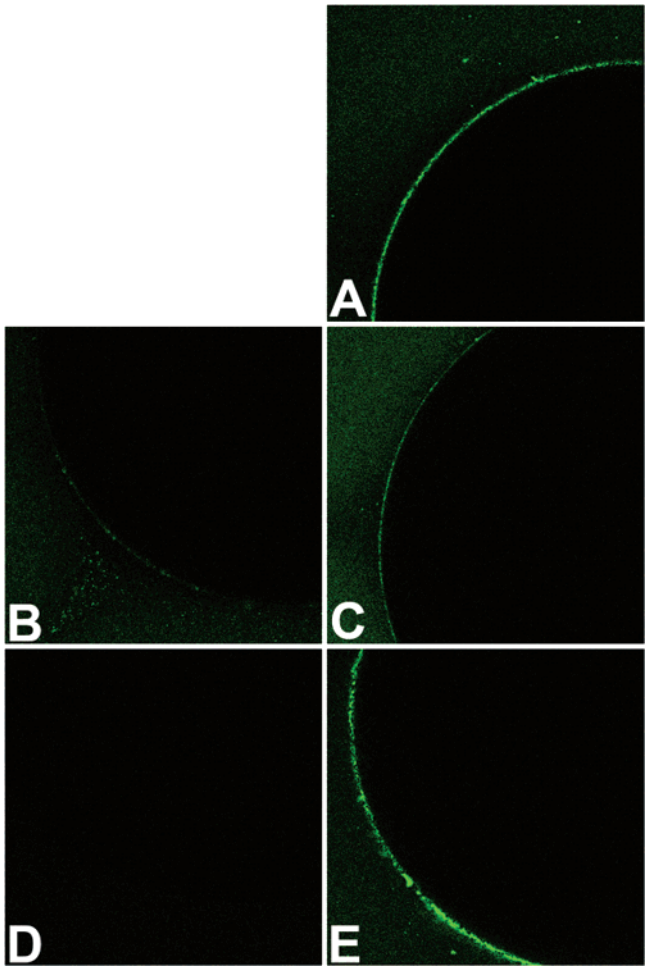

Figure 8. Two-phase experiments with qdot-containing structures and oocytes expressing human ρ1 $GABA_C$ receptors. (A) Positive control for this series of observations (oocyte expressing human ρ1, imaged after a 5-min incubation in 34 nM M−PEG−qdot). (B−C) Oocyte after two-phase incubation involving (1) 34 nM unconjugated qdot (B) and (2) 34 nM M−PEG−qdot in buffer supplemented with 34 nM unconjugated qdot (C). D−E: Oocyte after two-phase incubation involving (1) 34 nM PEG−qdot (D) and (2) 34 nM M−PEG−qdot in buffer supplemented with 34 nM PEG−qdot (E).

Generally similar results were obtained when human ρ1 $GABA_C$-expressing oocytes were treated with PEG−qdots, i.e., with qdots conjugated to PEG 2000 that lacked an (aminohexanoyl) muscimol terminating group (Figure 8D−E and Table 1, rows 12−13). ANOVA of the postphase 1 and postphase 2 fluorescence data yielded ($F(1, 1101) = 1324.40$, $p < 10^{-6}$, $\eta^2 = 0.55$; $\chi^2(3848) = 4138.6$, $p = 0.001$), i.e., indicated a significant increase in border intensity upon phase 2 incubation with M−PEG−qdots. As observed with unconjugated qdots, the postphase 1 border intensity with PEG−qdots was significantly lower than the border intensity of the positive control. However, by contrast with results obtained with unconjugated qdots, background fluorescence intensity obtained with PEG−qdots was small by comparison with that of the positive control. We interpret the low overall (i.e., both border and background) fluorescence obtained with PEG−qdots as due at least in part to a reduction in fluorescence quenching associated with the relatively high ligand loading of the PEG−qdot preparation (see Experimental Section).

The results of these experiments with unconjugated qdots and PEG−qdots argue against a nonspecific binding of the qdot moiety to $GABA_C$ receptors or other components of the oocyte surface membrane as the basis of the binding activity described in the experiments of Figures 4, 5, and 7.

B. Three-Phase Incubations. Figure 7 and the accompanying tabular and statistical data described above indicate that agonists such as GABA at ≥100 μM concentration, when coincubated with 34 nM M−PEG−qdots, significantly reduce the binding of M−PEG−qdots as determined at the end of the (second-phase) incubation. To investigate whether this competition with M−PEG−qdot binding is reversible, we employed a three-phase protocol in which the second incubation was followed by washing of the oocyte and a further incubation with 34 nM M−PEG−qdots only. Figure 9A shows the result obtained from the positive control ρ1-expressing oocyte investigated on the day of the experiment to be described. Figure 9B−C show results obtained from an oocyte subjected to a three-phase incubation involving treatment with 100 μM GABA. Image B, which was obtained at the end of the second-phase incubation (100 μM GABA plus 34 nM M−PEG−qdot), may be compared with image C obtained at the end of the third-phase incubation with 34 nM PEG−qdot alone. Two-way ANOVA of the Figure 9B−C data, using border and background measurements as within-sample measurements and condition/treatment as a between-sample measurement, indicated a significant increase in ratio of border-to-background intensity between the end of phase 2 and the end of phase 3 (Table 1, rows 14−15; 22.41 ± 32.71 vs 119.51 ± 84.47) ($F(1, 1229) = 679.95$, $p < 10^{-6}$, $\eta^2 = 0.36$). Furthermore, the border intensity at the conclusion of phase 3 was higher than that of the positive control (71.80 ± 77.62) ($F(1, 1100) = 100.22$, $p < 10^{-6}$, $\eta^2 = 0.08$), indicating essentially complete recovery of M−PEG−qdot binding. The relationship among the fluorescence data obtained at the end of phase 2 (Figure 9B), at the end of phase 3 (Figure 9C), and from the positive control (Figure 9A) is further described by the border and background distributions accompanying each image. For the border region, the distribution exhibited at the end of phase 3 barely reached the criterion for a significant difference with respect to the positive control. Furthermore, the border distribution exhibited at the end of phase 2 did not differ significantly from that exhibited at the end of phase 3; it did, however, differ markedly from that exhibited by the positive control ($\chi^2(21\,922) = 22\,373.75$, $p = 0.016$).

Results similar to those of the Figure 9 experiment were obtained in three-phase experiments involving treatment with 500 μM GABA or with 5 mM GABA (not illustrated). With 500 μM GABA, the ratio of border-to-background intensity obtained at the end of phase 3 (123.85 ± 84.67), i.e., in the presence of 34 nM M−PEG−qdots alone, differed significantly from that obtained at the end of phase 2 (44.43 ± 48.26), i.e., in the presence of both 500 μM GABA and 34 nM M−PEG−qdots (two-way ANOVA, $F(1, 1040) = 350.73$, $p < 10^{-6}$, $\eta^2 = 0.25$). With 5 mM GABA, there was a significant shift in border values between the end of phase 2 (30.32 ± 28.51) and the end of phase 3 (54.26 ± 37.35) (two-way ANOVA, $F(1, 1076) = 138.01$, $p < 10^{-6}$, $\eta^2 = 0.11$).

Discussion

The present study has examined the interaction of $GABA_C$ receptors with a conjugate synthesized from CdSe qdots, with the receptor agonist muscimol tethered distally in multiple copies

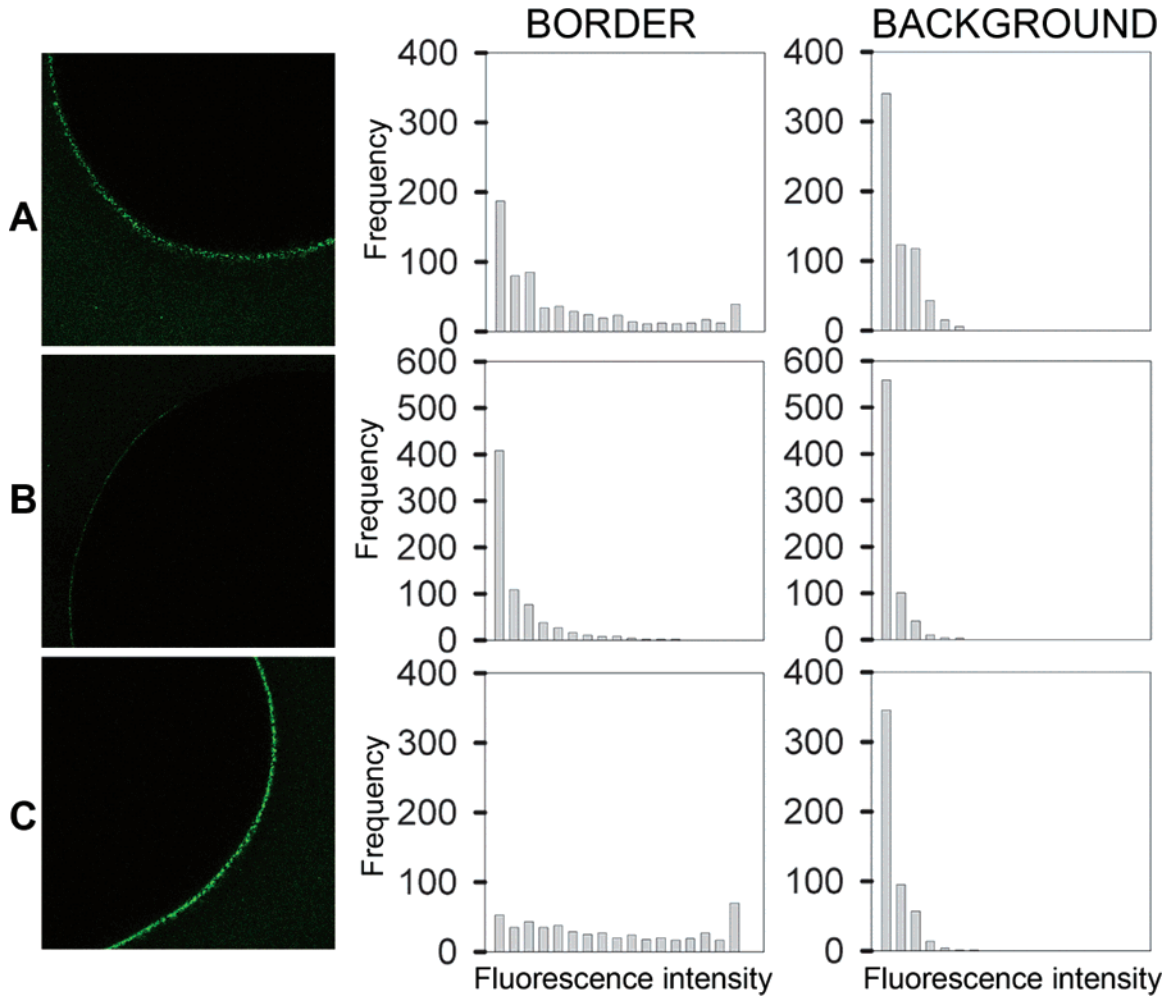

Figure 9. Three-phase experiment involving competition with 100 μM GABA. (A) Results obtained from a positive control oocyte (single-phase incubation with 34 nM M−PEG−qdot) examined on the same day as that of the experiments shown in B and C. (B−C) Fluorescence images obtained with three-phase incubation, and with 100 μM GABA as a test competitor. Data obtained from a single oocyte following the second-phase incubation (medium containing 100 μM GABA and 34 nM M−PEG−qdots) (B), and after the third-phase incubation (medium containing only 34 nM M−PEG−qdots) (C). Distributions describe fluorescence intensities for border and background regions of the corresponding fluorescence images.

to the qdot by a PEG linker. The primary finding is that the qdot-tethered form of muscimol investigated here exhibits specific binding to expressed $GABA_C$ receptors and that this binding activity depends on the presence of muscimol in the conjugate. Three types of evidence support this view. First, the compound binds selectively to oocytes expressing $GABA_C$ receptors. Second, results obtained from the two-phase experiments indicate an inhibition of M−PEG−qdot binding by GABA (>100 μM), muscimol (>100 μM), and M−PEG (500 μM) (i.e., a competition, by these agents, with M−PEG−qdot binding); an absence of substantial binding activity by structures lacking muscimol (unconjugated qdots and PEG−qdots); and little if any competition by the muscimol-lacking structures with the binding of M−PEG−qdots. Third, results of the three-phase experiments indicate that the removal of competing GABA restores the muscimol−PEG−qdot binding ability of the $GABA_C$ receptors. To our knowledge, the present study is the first to provide evidence for binding activity, at the ligand-binding pocket of a ligand-gated ion channel, of a receptor agonist covalently joined to a qdot.

The approach used here builds on that employed by Rosenthal et al.,[28] who synthesized a conjugate consisting of AMP-coated CdSe qdots covalently joined to serotonin through a short linker arm. In labeling, transport, and electrophysiological experiments employing this conjugate, Rosenthal et al.[28] found that the conjugate exhibits specific binding activity at human and drosophila serotonin transporters expressed in HeLa and HEK-293 cells and inhibits transport of serotonin in HeLa cells expressing serotonin transporters. The conjugate lacked electrophysiological activity on *Xenopus* oocytes expressing the serotonin receptor but, on oocytes expressing the serotonin transporter, exhibited activity similar to that of antagonists. Other investigators have used qdots coupled covalently to various other functional groups to target receptors in vitro and in vivo. Examples include the use of transferrin−qdot conjugates that underwent receptor-mediated endocytosis;[2] of lung-targeting peptide−qdot conjugates injected in vivo into the peripheral circulation;[19] of EGF−qdots to target receptor tyrosine kinase and quantify EGF binding and internalization;[20] and of peptide−qdot conjugates to image the angiotensin receptor.[49,50] In addition, streptavidin-coated qdots conjugated noncovalently with biotinylated biomolecules (e.g., biotinylated bombesin or

(49) Tomlinson, I. D.; Mason, J. N.; Blakely, R. D.; Rosenthal, S. J. *Methods Mol. Biol.* **2005**, *303*, 51−60.
(50) Mason, J. N.; Farmer, H.; Tomlinson, I. D.; Schwartz, J. W.; Savchenko, V.; DeFelice, L. J.; Rosenthal, S. J.; Blakely, R. D. *J. Neurosci. Methods* **2005**, *143*, 3−25.

angiotensin II) have recently been used to target G-protein-coupled receptors,[51] glial cells,[52] biomolecules such as single kinesins,[53] and specific proteins in living cells.[54] Other investigations have employed biotinylated antibodies or peptides conjugated with streptavidin-coated qdots as targeting agents.[23,55−57]

The design of the qdot-conjugated structure used in the present experiments was motivated by a recent study indicating that a chain-derivatized form of muscimol containing a sterically bulky biotin group ("muscimol−biotin") exhibits agonist activity at $GABA_C$ and $GABA_A$ receptors expressed in *Xenopus* oocytes.[46,58] Muscimol−biotin differs from the present M−PEG−qdot in that it contains muscimol conjugated to biotin through a short hydrocarbon (aminohexanoyl) linker, rather than to a qdot through a long PEG (plus aminohexanoyl) linker. Available data furthermore indicate an interaction between $GABA_A$ receptors in retinal neurons and muscimol conjugated to the bulky fluorophore BODIPY;[59] electrophysiological activity of muscimol−BODIPY at $GABA_A$ and $GABA_C$ receptors;[46] and high-affinity interaction between $GABA_A$ receptors of rat hippocampal neurons and muscimol conjugated to Alexa Fluor 532.[60] In light of the evident binding activity of the present qdot-based structure and the previous studies just summarized, we conclude that muscimol, when conjugated to a sterically bulky component (e.g., qdot or biotin) through a linker that avoids steric clash of this bulky component with the receptor, retains receptor-binding activity. The present results specifically demonstrate the ability of the long-chain PEG linker used here to permit binding of the muscimol moiety at the $GABA_C$ ligand-binding site, i.e., to achieve sufficient distance of the qdot platform from the $GABA_C$ binding pocket.

A striking property of the conjugate is the strength of its interaction with oocyte-expressed $GABA_C$ receptors. This interaction may depend in part on the presence of the PEG−qdot structure in the conjugate. As indicated by the wash-out experiments of Figure 6, half-reduction of the fluorescence signal due to membrane-bound M−PEG−qdots requires approximately 10−15 min of incubation following transfer into a ligand-free medium. Interestingly, electrophysiological data obtained with muscimol−biotin and muscimol−BODIPY at oocyte-expressed $GABA_C$ receptors indicate that the exponential time constant for recovery of the agonist response to these compounds substantially exceeds that for muscimol itself (about 15 s for muscimol−biotin and muscimol−BODIPY vs about 4 s for muscimol). As discussed by Vu et al.,[46] the relatively long recovery time course of the electrophysiological response to muscimol−biotin and muscimol−BODIPY may derive to some extent from an (as yet undetermined) interaction of the terminating biotin or BODIPY group conjugated to muscimol in these structures. Conceivably, the evident slowness of wash-out of M−PEG−qdots observed in the present fluorescence experiments could reflect a long-persisting interaction of the tethering qdot with the receptor. If this is the case, such a qdot/receptor interaction must depend on conjugation of the qdot with muscimol, as neither unconjugated qdots nor PEGylated qdots exhibit substantial binding (Figure 8 and Table 1). Previous studies have shown that quantum dots coated with an amphiphilic polymer shell bind nonspecifically to mammalian cell membranes. However, when these quantum dots are PEGylated, this nonspecific binding is significantly reduced.[29,49]

A further factor that may play a role in the affinity of the M−PEG−qdot for the $GABA_C$ receptor concerns its multivalency, since the conjugate contains an average of approximately 150−200 PEG−muscimol ligands coupled to each qdot. This multivalency can be expected to increase the effective concentration of muscimol locally available for interaction with neighboring $GABA_C$ ligand binding sites when the M−PEG−qdot is bound through at least one muscimol's binding. That is, the high avidity of the M−PEG−qdot structure is expected to promote retention of the M−PEG−qdot at the oocyte surface membrane and could contribute also to the evident time course of M−PEG−qdot wash-out (Figure 6). Interestingly, Lester et al.[61] found that a bivalent form of acetylcholine exhibits high binding activity to the acetylcholine receptor, a ligand-gated ion channel of structure generally similar to that of $GABA_A$ and $GABA_C$ receptors. Studies by Kula et al.[62] and by Lin and Licht[63] have shown that other Y-shaped or bivalent ligands also exhibit activity at acetylcholine receptors. These considerations, together with the presence of multiple ligand-binding sites on the pentameric receptor[64] and evidence for the cooperativity of ligand binding to GABA receptors,[31] are consistent with the occurrence of a specific affinity of M−PEG−qdots for the receptor.

In conclusion, the present findings describe the specific recognition, by a neurotransmitter membrane receptor, of a multivalent agonist-containing structure in which the multiple copies of receptor ligand are tethered to a sterically bulky distal component (here, the qdot) through a suitably long linker. The evident binding activity of this type of conjugate in the present $GABA_C$ system raises the possibility that a sterically bulky structure of nanometer or larger scale positioned at or near the receptor's extracellular surface could control receptor activity by governing the access, to receptor binding pockets, of ligands tethered to the external structure. The present findings thus encourage the investigation of such structures for possible applications in the control or modulation of neural signaling.

Acknowledgment. The authors thank Ms. Ruth Zelkha for her expert assistance with cell imaging and fluorescence analysis, Mr. Niraj J. Muni for oocyte preparation, Dr. Robert F. Standaert for helpful discussions, and Quantum Dot Corporation for providing the AMP-coated quantum dots used in this study. Supported by NIH Grants EY13693, EY016094, EY05494, EY01792, EB003728, EM72048, and MH075791; by a grant

(51) Young, S. H.; Rozengurt, E. *Am. J. Physiol. Cell Physiol.* **2006**, *290*, C728−C732.
(52) Pathak, S.; Cao, E.; Davidson, M. C.; Jin, S.; Silva, G. A. *J. Neurosci.* **2006**, *26*, 1893−1895.
(53) Seitz, A.; Surrey, T. *EMBO J.* **2006**, *25*, 267−277.
(54) Howarth, M.; Takao, K.; Hayashi, Y.; Ting, A. Y. *Proc. Natl. Acad. Sci. U.S.A.* **2005**, *102*, 7583−7588.
(55) Mason, J. N.; Tomlinson, I. D.; Rosenthal, S. J.; Blakely, R. D. *Methods Mol. Biol.* **2005**, *303*, 35−50.
(56) Vu, T. Q.; Maddipati, R.; Blute, T. A.; Nehilla, B. J.; Nusblat, L.; Desai T. A. *Nano Lett.* **2005**, *5*, 603−607.
(57) Yang, L.; Li, Y. *Analyst* **2006**, *131*, 394−401.
(58) Nehilla, B. J.; Popat, K. C.; Vu, T. Q.; Chowdhury, S.; Standaert, R. F.; Pepperberg, D. R.; Desai, T. A. *Biotechnol. Bioeng.* **2004**, *87*, 669−674.
(59) Wang, H.; Standifer, K. M.; Sherry, D. M. *Visual Neurosci.* **2000**, *17*, 11−21.
(60) Meissner, O.; Häberlein, H. *Biochemistry* **2003**, *42*, 1667−1672.
(61) Lester, H. A.; Chabala, L. D.; Gurney, A. M.; Sheridan, R. E. *Soc. Gen. Physiol. Ser.* **1986**, *40*, 447−462.
(62) Kula, M. A.; Dunn, S. M. J.; Dryden, W. F. *2004 Annual Meeting of the Society for Neuroscience* **2004**, Program Number 624.20 (abstr.).
(63) Lin, W. C.; Licht, S. *2006 Annual Meeting of the Biophysical Society* **2006**, Program Number 56 (abstr.).
(64) Chang, Y.; Weiss, D. S. *Nat. Neurosci.* **1999**, *2*, 219−225.

from the University of Illinois Intercampus Research Initiative in Biotechnology Program; by a Macular Degeneration Research grant from the American Health Assistance Foundation (Clarksburg, MD); and by an unrestricted departmental award from Research to Prevent Blindness (New York, NY). D.R.P. is a Senior Scientific Investigator of Research to Prevent Blindness. Preliminary results were presented at the 2005 and 2006 Annual meetings of the Association for Research in Vision and Ophthalmology.

Supporting Information Available: Further experimental details on the photophysical properties of the muscimol-conjugated qdots (Figures S1−S3 and movie file). This material is available free of charge via the Internet at http://pubs.acs.org.

JA064324K